

Multiple Functions of Sterols in Yeast Endocytosis

Antje Heese-Peck,^{*†} Harald Pichler,^{*} Bettina Zanolari,^{*} Reika Watanabe,^{*} Günther Daum,[‡] and Howard Riezman^{*§}

^{*}Biozentrum, University of Basel, CH-4056 Basel, Switzerland; and [‡]Institut für Biochemie, Technische Universität, A-8010 Graz, Austria

Submitted April 5, 2002; Revised May 21, 2002; Accepted May 31, 2002
Monitoring Editor: Hugh R.B. Pelham

Sterols are essential factors for endocytosis in animals and yeast. To investigate the sterol structural requirements for yeast endocytosis, we created a variety of *ergΔ* mutants, each accumulating a distinct set of sterols different from ergosterol. Mutant *erg2Δerg6Δ* and *erg3Δerg6Δ* cells exhibit a strong internalization defect of the α -factor receptor (Ste2p). Specific sterol structures are necessary for pheromone-dependent receptor hyperphosphorylation, a prerequisite for internalization. The lack of phosphorylation is not due to a defect in Ste2p localization or in ligand-receptor interaction. Contrary to most known endocytic factors, sterols seem to function in internalization independently of actin. Furthermore, sterol structures are required at a postinternalization step of endocytosis. *ergΔ* cells were able to take up the membrane marker FM4-64, but exhibited defects in FM4-64 movement through endosomal compartments to the vacuole. Therefore, there are at least two roles for sterols in endocytosis. Based on sterol analysis, the sterol structural requirements for these two processes were different, suggesting that sterols may have distinct functions at different places in the endocytic pathway. Interestingly, sterol structures unable to support endocytosis allowed transport of the glycosylphosphatidylinositol-anchored protein Gas1p from the endoplasmic reticulum to Golgi compartment.

INTRODUCTION

Cells use endocytosis to take up extracellular nutrients, regulate membrane dynamics, and respond to extracellular stimuli by desensitizing, down-regulating, or recycling of receptors and transporters. In receptor-mediated endocytosis, a ligand binds specifically to its receptor at the plasma membrane, leading to its internalization into small endocytic vesicles. These receptors move through an early and late endosomal compartment to a degradative organelle or recycle to the plasma membrane. Genetic screens, most successful in yeast, and biochemical approaches have led to the identification of internalization signals and components of the endocytic machinery (Geli and Riezman, 1998; D'Hondt *et al.*, 2000).

In addition to proteinaceous factors, lipids have emerged as important regulators of internalization. These include phosphoinositides for protein recruitment (Corvera *et al.*, 1999), sphingoid bases (precursors of sphingolipids) as signaling molecules for protein phosphorylation (Friant *et al.*, 2000; Zanolari *et al.*, 2000), and phosphatidic acid for mem-

brane curvature (Schmidt *et al.*, 1999). Sterols, mainly found in the plasma membrane, play a role in endocytosis (Heiniger *et al.*, 1976). In animal cells, cholesterol depletion interferes with internalization of proteins in raft domains, as defined by their insolubility in cold detergent (Chang *et al.*, 1992; Parton *et al.*, 1994; Deckert *et al.*, 1996; Orlandi and Fishman, 1998). However, cholesterol depletion does not always have this effect (Mayor *et al.*, 1998). Cholesterol has also been reported to be required for internalization through clathrin-coated pits that do not display raft characteristics (Rodal *et al.*, 1999; Subtil *et al.*, 1999). Furthermore, several studies indicate that cellular levels of cholesterol affect the movement of proteins through endosomal compartments (Mayor *et al.*, 1998; Grimmer *et al.*, 2000).

The identification of *ERG2* as *END11*, isolated as an endocytosis mutant (Munn and Riezman, 1994), has provided the first indication that sterols are required for endocytosis in yeast (Munn *et al.*, 1999). *ERG2* encodes the C-8 sterol isomerase, an enzyme in the ergosterol biosynthetic pathway. *erg2Δ* cells accumulate sterols different from ergosterol and exhibit reduced internalization levels of the α -factor receptor (Ste2p) (Munn and Riezman, 1994; Munn *et al.*, 1999). The creation of additional *erg* mutants (*erg6Δ* and *erg2Δerg6Δ*), accumulating distinct sets of sterols, allowed us to begin to examine the structural requirement for sterols in receptor-mediated endocytosis *in vivo* without the use of drugs for sterol depletion. *erg6Δ* and *erg2Δerg6Δ* also

Article published online ahead of print. Mol. Biol. Cell 10.1091/mbc.E02-04-0186. Article and publication date are at www.molbiolcell.org/cgi/doi/10.1091/mbc.E02-04-0186.

[†] Current address: Sainsbury Laboratory, John Innes Center, Colney Lane, Norwich NR4 7UH, England.

[§] Corresponding author. E-mail address: howard.riezman@unibas.ch.

Table 1. Strains used in this study

Strain	Genotype	Source
RH448	<i>MATa leu2 ura3 his4 lys2 bar1</i>	Lab strain
RH1201	<i>MATa/MATα leu2/leu2 ura3/ura3 his4/his4 lys2/lys2 bar1/bar1</i>	Lab strain
RH1298	<i>MATa ste2Δ::LEU2 leu2 ura3 his4 bar1</i>	Lab strain
RH2897	<i>MATa erg2(end11)-1Δ::URA3 leu2 ura3 his4 lys2 bar1</i>	Munn <i>et al.</i> (1999)
RH2950	<i>MATa rvs167Δ::TRP1 leu2 ura3 trp1::URA3 his4 bar1</i>	Lab strain
RH3589	<i>MATa yck1Δ yck2-2 leu2 ura3 his3 ade2 bar1</i>	Hicke <i>et al.</i> (1998)
RH3616	<i>MATa erg2(end11)-1Δ::URA3 erg6Δ leu2 ura3 bar1</i>	Munn <i>et al.</i> (1999)
RH3622	<i>MATa erg6Δ::LEU2 leu2 ura3 his4 bar1</i>	Munn <i>et al.</i> (1999)
RH3919	<i>MATα erg5Δ::kanMX4 leu2 ura3 his4 lys2 bar1</i>	This study
RH3920	<i>MATa/MATα erg5Δ::kanMX4/ERG5 leu2/leu2 ura3/ura3 his4/his4 lys2/lys2 bar1/bar1</i>	This study
RH4213	<i>MATa erg3Δ::LEU2 leu2 ura3 his4 lys2 bar1</i>	This study
RH4214	<i>MATα erg3Δ::LEU2 leu2 ura3 his4 lys2 bar1</i>	This study
RH4216	<i>MATa/MATα erg4Δ::URA3/ERG4 leu2/leu2 ura3/ura3 his4/his4 lys2/lys2 bar1/bar1</i>	This study
RH4217	<i>MATa erg4Δ::URA3 leu2 ura3 his4 lys2 bar1</i>	This study
RH4803	<i>MATa/MATα erg3Δ::LEU2/ERG3 leu2/leu2 ura3/ura3 his4/his4 lys2/lys2 bar1/bar1</i>	This study
RH5225	<i>MATa erg3Δ::LEU2 erg6Δ::LEU2 leu2 ura3 his4 lys2 bar1</i>	This study
RH5227	<i>MATa/MATα erg2Δ(end11)-1Δ::URA3/ERG2 erg3Δ::LEU2/ERG3 leu2/leu2 ura3/ura3 his4/his4 lys2/lys2 bar1/bar1</i>	This study
RH5228	<i>MATa erg2(end11)-1Δ::URA3 erg3Δ::LEU2 leu2 ura3 his4 lys2 bar1</i>	This study
RH5231	<i>MATa/MATα erg4Δ::URA3/ERG4 erg5Δ::kanMX4/ERG5 leu2/leu2 ura3/ura3 his4/his4 lys2/lys2 bar1/bar1</i>	This study
RH5233	<i>MATa erg4Δ::URA3 erg5Δ::kanMX4 leu2 ura3 his4 lys2 bar1</i>	This study
RH5297	<i>MATa end3Δ::kanMX4 leu2 ura3 his3 trp1 bar1</i>	Lab strain

showed defects in receptor-mediated internalization, with *erg2 Δ erg6 Δ* cells having the most severe block (Munn *et al.*, 1999). Analyses of these three *erg Δ* mutants indicated that the severity of the internalization defect may correlate with changes in the sterol structure. The main sterol in *erg2 Δ erg6 Δ* cells is zymosterol, which contains a single desaturation at C-8,9 and lacks the side-chain methylation at C-24,28, implying that the desaturation state of the sterol B-ring is of importance, in particular because *erg6 Δ* cells, which lack the side-chain methylation at C-24,28, had a weaker defect in internalization (Munn *et al.*, 1999). Sterols also function in fluid-phase endocytosis because vacuolar accumulation of the water-soluble dye lucifer yellow (LY) was blocked in *erg2 Δ* and *erg2 Δ erg6 Δ* cells.

Although sterols are clearly important factors for yeast endocytosis, it is unknown at which step(s) these lipids function. In the past, studies using Ste2p, a G protein-coupled receptor involved in the mating response, as an endocytic marker protein have been very fruitful in dissecting the requirements for ligand-induced internalization (Geli and Riezman, 1998; Riezman, 1998). In the absence of its ligand, Ste2p undergoes slow constitutive endocytosis, but its internalization rate is greatly stimulated in response to binding of its ligand, α -factor (Riezman, 1998). On α -factor binding, Ste2p becomes hyperphosphorylated on its cytoplasmic tail (Reneke *et al.*, 1988). Hyperphosphorylation is required for subsequent ubiquitination at surrounding lysines (Hicke *et al.*, 1998). Ubiquitin serves as the actual internalization signal because mono-ubiquitination is sufficient to drive Ste2p internalization (Terrell *et al.*, 1998; Shih *et al.*, 2000), and the three-dimensional structure of ubiquitin seems to carry the internalization signal (Shih *et al.*, 2000). Another requirement that acts subsequent to receptor modification is a dynamic actin cytoskeleton. In yeast, many proteins that function in internalization are involved in building or regulating the

actin cytoskeleton (Geli and Riezman, 1998; D'Hondt *et al.*, 2000).

Herein, we show a sterol structural requirement for receptor-mediated endocytosis at or before hyperphosphorylation of Ste2p. Furthermore, we provide evidence that specific sterol structures most likely have additional roles at postinternalization steps in endocytosis.

MATERIALS AND METHODS

Yeast Media, Strains, and Genetic and DNA Techniques

For all experiments, medium was inoculated directly from plates with colonies that were not older than 2 wk. Unless otherwise mentioned, cells were grown overnight at 24°C to $0.4\text{--}1.0 \times 10^7$ cells/ml in rich medium (YPUADT) (Munn *et al.*, 1999). Standard yeast genetic techniques and DNA manipulations were performed as described and referenced previously (Munn *et al.*, 1999). Recombinant lyticase was purified from *Escherichia coli* as described previously (Hicke *et al.*, 1997).

Yeast strains used in this study are listed with their relevant phenotypes in Table 1. All *erg* mutants were isogenic and made in the diploid RH1201. The heterozygous diploid strains RH4803 and RH4216 were generated by replacing one genomic copy of *ERG3* or *ERG4* in RH1201 with the selectable marker *LEU2* or *URA3*, respectively. The *ERG3* deletion cassette was amplified by polymerase chain reaction (PCR) from YDp-L (Berben *et al.*, 1991) with the oligonucleotides *ERG3-1s* (5' GTA AAA AAA GAT AAT AAG AAA AAT ATT CGT CTA GAT GTT AGA ATT CCC GGG GAT CCG C 3') and *ERG3-2a* (5' CTT GAA CGT GAA AGA AAG AAA AAA GAT GAG ACA AAC AAG GAA GCT AGC TTG GCT GCA G 3'). The same strategy was used to create RH4216 by using the oligonucleotides *ERG4-1s* (GAT ACG GAT ATT TAC GTA GTG TAC ATA GAT TAG CAT CGC TGA ATT CCC GGG GAT CCG C 3') and *ERG4-2a* (5' AGC CCT TTT GTC GCG TAA ATA CAT CAA TAC TTT TAT ATA CAA GCT AGC TTG GCT GCA G 3').

The heterozygous diploid strain RH3920 was generated by replacing one genomic copy of *ERG5* in RH1201 with a deletion cassette containing a kanMX4-module, which was constructed using Long-Flanking Homology PCR (Wach, 1996) and the following primers: ERG5-L1s (5' CGC ATA TGG GCG CCC ACA CC 3'), ERG5-L2a (5' GGG GAT CCG TCG ACC TGC AGC GTA CCA TTT TGT TAA AAG GTA TTT ATT GTC TAT TGG 3'), ERG5-L3s (5' AAC GAG CTC GAA TTC ATC GAT GAT ATG ATG GGG AAA AAC GAG ACT TTG TCC AG 3'), and ERG5-L4a (5' GCT GTC ATG CTC GCC TTC ACG 3'). Homologies to *ERG* genes are indicated in bold, and homology to the Ydp- or pFA6a-kanMX4 plasmids are in normal lettering.

The haploid strains RH4213 and RH4214 were generated from RH4803, RH4217 from RH4216, and RH3919 from RH3920. RH3622 and RH4214 were crossed to generate RH5225. Replacement of both *ERG3* and *ERG6* genes was confirmed by PCR. Strains RH4214 and RH2897 or RH4217 and RH3919 were crossed to create RH5227 or RH5231, which were used to generate RH5228 or RH5233, respectively.

Endocytosis Assays and Vacuole Acidification

Internalization assays were carried out at 37°C using the continuous presence protocol with a 15-min preshift to 37°C before adding the [³⁵S]α-factor (Dulic *et al.*, 1991). Internalization (in percentage) was calculated by dividing internalized counts (pH1-resistant counts) by the total cell-associated counts (pH6-resistant counts) for each time point. Values correspond to the means of three or four experiments. The [³⁵S]α-factor was prepared as described previously (Dulic *et al.*, 1991). For fluid-phase endocytosis, cells were incubated with lucifer yellow carbohydrazide (dilithium salt; Fluka AG, Buchs, Switzerland) and processed for fluorescence microscopy as described previously (Munn *et al.*, 1999).

N-[3-Triethylammoniumpropyl]-4-[*p*-diethylaminophenyl]hexatrienyl pyridinium dibromide (FM4-64) staining was performed as described previously (Wiederkehr *et al.*, 2000) with minor modifications. Cells grown to early logarithmic phase were resuspended in fresh YPUADT to 2 × 10⁶ cells/ml and incubated with FM4-64 (Molecular Probes, Eugene, OR) at a final concentration of 20 μM on ice for 30 min. Cells were then washed twice with ice-cold YPUADT. Internalization of FM4-64 was started by addition of YPUADT (24°C). Aliquots were taken at 15, 30, 45, and 180 min, washed twice with ice-cold YPUADT containing 15 mM each of sodium azide and sodium fluoride. Samples were examined using tetramethylrhodamine B isothiocyanate filter set and Nomarski optics using an Axioplan2 fluorescence microscope (Carl Zeiss, Thornwood, NY). All images were processed identically with the exception that exposure times for fluorescence images were 8 s for 15-, 30-, and 45-min time points and 4 s for 180-min time points, respectively.

Detection of acidified vacuoles was performed using quinacrine and fluorescence microscopy on cells grown in YPUADT medium according to previously published methods (Weisman *et al.*, 1987; Rothman *et al.*, 1989).

Rhodamine-Phalloidin Staining of Actin

Cells at a density of 1 × 10⁷ cells/ml were incubated for 2.5–3 h at 37°C, fixed in formaldehyde, and stained with rhodamine-phalloidin (Sigma-Aldrich) to visualize F-actin essentially as described previously (Kilmartin and Adams, 1984). All images were processed identically.

Hyperphosphorylation and Ubiquitination of Ste2p

Treatment and preparation of cell lysates was modified from a previous protocol (Hicke and Riezman, 1996). Cells were harvested, resuspended to 2.5 × 10⁷ cells/ml in prewarmed YPUADT, and preincubated at 37°C for 15 min, during which cycloheximide was added to 10 μg/ml for the final 10 min. An aliquot of 5 × 10⁷ cells

(0-min time point) was removed to a tube on ice containing NaF/NaN₃ (20 mM final concentration each). α-Factor (Sigma-Aldrich) was added to 1 × 10⁻⁷ M to the remaining cells. Aliquots were removed at 8 and 16 min after α-factor addition, transferred to tubes on ice containing NaF/NaN₃, and incubated for at least 10 min. Cell lysates were prepared as described previously (Hicke and Riezman, 1996) except that cells were broken using a bead beater (2 × 45-s pulses at level 6.5; FastPrep; Bio101, Savant, Hollbrook, NY) at 4°C. For each time point, extracts from ~1 × 10⁷ cells were separated on SDS-PAGE and transferred to nitrocellulose. Because of the high abundance of unmodified Ste2p, material from only 0.5 × 10⁷ cells were loaded for *yck-ts* cells. Blots were blocked in phosphate-buffered saline (PBS) containing 10% milk for 1–2 h at room temperature followed by incubation with anti-Ste2p antiserum (1:500 dilution) in PBS/10% milk overnight at 4°C. Blots were washed with PBS/0.025% Tween 20/0.025% Triton X-100 and with PBS. After incubation with goat anti-rabbit IgG-coupled peroxidase (1:5000 dilution; Sigma-Aldrich) in PBS/10% milk, blots were washed as described above and developed with the ECL chemiluminescence detection system (Amersham Biosciences, Piscataway, NJ).

Immunofluorescence Microscopy

Cells (2 × 10⁸) were harvested and shifted to 37°C for 15 min. Cycloheximide was added to 20 μg/ml for the final 10 min. Cells were fixed by addition of 0.1 volume of 37% formaldehyde/1 M potassium phosphate, pH 6.5, for 1.5–2 h and further processed (Hicke *et al.*, 1997). Fixed cells were incubated with purified anti Ste2p-antiserum (1:10 dilution) followed by Cy3-conjugated secondary goat anti-rabbit antibody (1:800 dilution; Molecular Probes) and prepared for immunofluorescence microscopy (Hicke *et al.*, 1997). To obtain comparable signals, images of *ste2Δ*, *erg2Δerg6Δ* and *erg3Δerg6Δ* cells were exposed twice as long as for wild type (WT) and *rvs167Δ*; otherwise, all images were processed identically.

Preparation of Anti-Ste2p Antibodies

Anti-Ste2p antibodies were raised in rabbits injected with a trpE-Ste2p fusion protein that contained the 100 N-terminal residues of Ste2p (Konopka *et al.*, 1988). Antibody specificity was assessed by protein blot analysis or immunofluorescence microscopy comparing protein extracts or cells, respectively, of RH448 (*STE2*) and RH1298 (*ste2Δ*). For immunofluorescence microscopy, the antiserum was purified by depletion of chitin antibodies by passing the antiserum twice over chitin columns (Schaerer-Brodbeck and Riezman, 2000).

Solubilization and Transport of Gas1p

Cells (1 × 10⁹) were washed, resuspended in 700 μl of TNE (50 mM Tris-HCl pH 7.4, 150 mM NaCl, 5 mM EDTA, and protease inhibitor cocktail; Sigma-Aldrich), and disrupted with glass beads. Cell debris and glass beads were removed by centrifugation at 500 × *g* for 5 min at 4°C. Equal volumes of TNE or TNE containing 2% Triton X-100 were added to the supernatant, incubated on ice for 1 h and centrifuged at 100,000 × *g* for 1 h at 4°C. The resulting pellet and supernatant fractions were subjected to SDS-PAGE and analyzed by Western blot analysis by using anti-Gas1p antibodies (1:10,000 dilution).

For Gas1p maturation studies, cells were grown overnight in SDYE (Dulic *et al.*, 1991) at 24°C to a final density of 0.7–1.0 × 10⁷ cells/ml. Analysis of Gas1p transport was essentially performed as described previously (Sutterlin *et al.*, 1997) with a 15-min preincubation and then pulse labeling and chase at 37°C.

α-Factor Competition

Cells were collected, washed in YPUADT, resuspended to 1 × 10⁹ cells/ml (mutant) or 0.25 × 10⁹ cells/ml (WT) in prewarmed (37°C) YPUADT containing 10 μg/ml cycloheximide, 10 mM *N*-*p*-tosyl-L-arginine methyl ester (Sigma-Aldrich), 20 mM NaF, 20 mM NaN₃,

and preincubated at 37°C for 15 min. The cell concentration was adjusted, so that ~10% of the radiolabeled α -factor was bound. 80 μ l of the cell suspension was added to prewarmed 20 μ l YPUADT/10 mM *N*-*p*-tosyl-L-arginine methyl ester containing 17×10^{-9} M radiolabeled α -factor (~10,000 cpm) as determined by halo-assay (Jenness *et al.*, 1983) and increasing amounts (10^{-9} – 10^{-6} M) of synthetic α -factor (Primm srl, Milan, Italy). The mixture was incubated at 37°C for 30 min and unbound α -factor was removed by filtering the cells (Dulic *et al.*, 1991). The amount of bound α -factor was determined by counting the filters in a scintillation counter.

Sterol Analysis

Collected cells were incubated for 30 min at 37°C. Total sterols were extracted from whole cells and analyzed by gas liquid chromatography (GLC) (Hewlett Packard 5 column) and GLC-mass spectrometry (MS) (Hewlett Packard 5-MS column) (Munn *et al.*, 1999). The abundance of each sterol was based on two independent experiments analyzed in duplicate by GLC.

RESULTS

Changes in Sterol Composition Can, but Do Not Necessarily, Lead to Internalization Defects

The five last steps of ergosterol synthesis, carried out by the *ERG2* through *ERG6* gene products (Figure 1), are not essential for viability of yeast. For the present studies, we created isogenic *erg* Δ single and double mutant strains that accumulated sterols with structural features different than those examined previously (Table 2) (Munn *et al.*, 1999). Based on their endocytic phenotypes, we focused herein on *erg3* Δ , *erg4* Δ *erg5* Δ , *erg2* Δ *erg3* Δ , and *erg3* Δ *erg6* Δ deletion strains. *erg3* Δ and *erg4* Δ *erg5* Δ cells grew at nearly WT rates at 24 or 37°C, whereas *erg2* Δ *erg3* Δ and *erg3* Δ *erg6* Δ cells grew at reduced rates at 24 and 37°C. Their slow-growth phenotype was, however, not as severe as that of *erg2* Δ *erg6* Δ cells (Munn *et al.*, 1999). Before further endocytic analyses, we determined the sterol compositions of the individual *erg* Δ strains. Total sterols were isolated from whole yeast cells under the same growth conditions used for the endocytic assays and separated by GLC and GLC-MS (Munn *et al.*, 1999). Sterols were identified based on their retention time and mass spectrum, and the relative abundance of each sterol was determined within a strain (Table 2). Consistent with our previous observation (Munn *et al.*, 1999), no significant differences were observed whether sterols were isolated after incubation at 24 or 37°C (our unpublished observations; Table 2). Overall, the sterol composition of each *erg* Δ strain was in agreement with the disruption of the various *ERG* genes leading to the absence of the respective enzyme activities and with the fact that ergosterol biosynthetic enzymes can act on a range of sterol substrates (Bard *et al.*, 1977; Smith and Parks, 1993; Daum *et al.*, 1998). None of the *erg* Δ cells contained ergosterol consistent with studies showing that yeast cells are unable to internalize sterols from the extracellular media under aerobic conditions (Trocha and Sprinson, 1976; Keesler *et al.*, 1992). This sterol exclusion prevented us from performing sterol feedback experiments under conditions required for endocytic assays (Munn *et al.*, 1999).

Using α -factor uptake assays, internalization by receptor-mediated endocytosis was quantified in *erg* Δ cells and compared with WT at 37°C. After addition of radiolabeled α -factor, the rate of internalization of the Ste2p-ligand complex

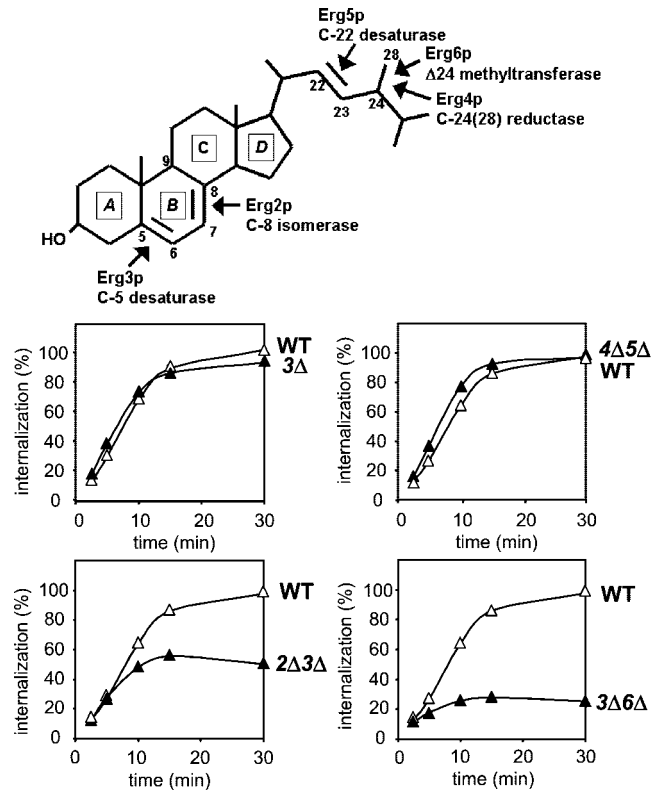


Figure 1. Analysis of α -factor internalization in *erg* mutants. A molecule of ergosterol is shown indicating the Erg proteins and their functions, whose corresponding genes have been inactivated in this study. Internalization assays were performed at 37°C on wild-type (WT, RH448), *erg3* Δ (3 Δ , RH4213), *erg2* Δ *erg3* Δ (2 Δ 3 Δ , RH5228), *erg3* Δ *erg6* Δ (3 Δ 6 Δ , RH5225), and *erg4* Δ *erg5* Δ (4 Δ 5 Δ , RH5233) cells. WT, closed triangles; mutant, open triangles.

was determined (Figure 1). Pheromone internalization was only partially defective in *erg2* Δ *erg3* Δ cells, but was almost completely defective in *erg3* Δ *erg6* Δ cells. This endocytic block was as severe as that observed for *erg2* Δ *erg6* Δ cells (Munn *et al.*, 1999) and the tightest yeast *end* mutants blocked in internalization, such as *myo5*, *cmd1* (Geli *et al.*, 1998), *end3*, *end4* (Raths *et al.*, 1993), *rvs167* Δ , *end6-1*/*rvs161* (Munn *et al.*, 1995), and *act1* (Kubler and Riezman, 1993). Interestingly, *erg3* Δ and *erg4* Δ *erg5* Δ cells did not exhibit any obvious defect in pheromone internalization, indicating that changes in the sterol composition do not necessarily lead to an internalization defect.

erg Δ Cells Do Not Show Any Obvious Perturbation of Actin Cytoskeleton Organization

All of the previously characterized *end* mutants with a general defect at the internalization step display an abnormal actin organization (D'Hondt *et al.*, 2000; Geli and Riezman, 1998). Therefore, we examined actin cytoskeleton organization in the *erg* Δ cells. WT and *erg* Δ cells were grown at 24°C and shifted to 37°C for 2.5–3 h. Cells were fixed, stained for F-actin using rhodamine-phalloidin, a method commonly

Table 2. Analysis of the sterol composition and the relative abundance of sterols within wild-type (WT, RH448), *erg3Δ* (RH4213), *erg2Δerg3Δ* (RH5228), *erg3Δerg6Δ* (RH5225), *erg4Δerg5Δ* (RH5233), *erg2Δ* (RH2897), *erg6Δ* (RH3622), and *erg2Δerg6Δ* (RH3616) cells.

Sterol	% Sterol	Mass
WT		
Zymosterol	6.9	384
Ergosterol	77.0	396
Tecosterol	3.0	398
A	5.1	398
Episterol	3.2	398
Lanosterol	3.8	426
4,4-dm-Cholesta-8,24-dienol	0.7	412
<i>erg2Δ</i>		
Squalene	1.4	410
Zymosterol	5	384
Ergosta-5,8,22-trienol	12.7	396
Ergosta-8,22-dienol	4.3	398
Fecosterol	33.2	398
Ergosta-8-enol	35.4	400
B	1.6	396
4-m-Cholesta-8,24-dienol	2.5	398
Lanosterol	2.9	426
4,4-dm-Cholesta-8,24-dienol	1.1	412
<i>erg3Δ</i>		
Zymosterol	2.9	384
Ergosta-8,22-dienol	4.1	398
Ergosta-7,22-dienol	45.9	398
Fecosterol	9.6	398
Ergosta-8-enol	7.8	400
Episterol	13.3	398
Ergosta-7-enol	10.8	400
Lanosterol	4.6	426
4,4-dm-Cholesta-8,24-dienol	1.0	412
<i>erg6Δ</i>		
Squalene	1.3	410
Cholesta-5,8,24-trienol	2.8	382
Zymosterol	39.4	384
Cholesta-5,7,24-trienol	32.3	382
Cholesta-7,24-dienol	7.7	384
Cholesta-5,7,22,24-tetraenol	7.9	380
C	2.7	398
Lanosterol	3.1	426
4,4-dm-Cholesta-8,24-dienol	2.3	412
<i>erg2Δerg3Δ</i>		
Squalene	1.7	410
D	2.0	386
Zymosterol	1.7	384
Ergosta-8,22-dienol	6.1	398
Fecosterol	39.3	398
Ergosta-8-enol	40.4	400
B	1.7	396
4-m-Cholesta-8,24-dienol	2.4	398
Lanosterol	3.1	426
4,4-dm-Cholesta-8,24-dienol	1.2	412
<i>erg3Δerg6Δ</i>		
Squalene	4.1	410
D	1.7	386
Zymosterol	40.9	384
Cholesta-7,24-dienol	39.5	384
C	5.2	398
Lanosterol	5.0	426
4,4-dm-Cholesta-8,24-dienol	3.4	412

Table 2 (continued).

Sterol	% Sterol	Mass
<i>erg2Δerg6Δ</i>		
Squalene	2.7	410
Zymosterol	85.6	384
E	3.7	382
4-m-Cholesta-8,24-dienol	1.5	398
Lanosterol	3.3	426
4,4-dm-Cholesta-8,24-dienol	2.1	412
<i>erg4Δerg5Δ</i>		
Zymosterol	7.2	384
Ergosta-5,8,24-trienol	2.6	396
Fecosterol	5.0	398
Ergosta-5,7,24-trienol	72.2	396
F	3.1	396
Lanosterol	8.9	426
4,4-dm-Cholesta-8,24-dienol	1.1	412

Data for RH2897, RH3622, and RH3616 from Munn *et al.* (1999).
m, methyl; dm, dimethyl. A–F, identification of sterols uncertain.

used to show defects in actin cytoskeleton organization in *end* mutants (Geli and Riezman, 1998), and observed by fluorescence microscopy (Figure 2). A shift from 24–37°C is known to induce a heat-induced reorganization of the actin cytoskeleton (Kilmartin and Adams, 1984), but this perturbation is transient and normal polarized actin organization is restored in WT cells within 2.5 h. In *erg2Δerg6Δ* and *erg3Δerg6Δ* cells, the actin cytoskeleton was arranged similarly to that of WT cells in that emerging daughter cells contained most of the cortical actin patches. Similar to WT cells, actin cables were clearly visible in some *ergΔ* cells. Comparable results were obtained for *erg3Δ* and *erg4Δerg5Δ* cells (our unpublished observations). In a control experiment, the actin cytoskeleton was delocalized in cells lacking a functional *Rvs167p*, a protein required for endocytic internalization and actin cytoskeleton organization (Bauer *et al.*, 1993; Lombardi and Riezman, 2001). In contrast to *ergΔ* and WT cells, *rvs167Δ* cells lacked visible actin cables, and their cortical actin patches were distributed over both the mother and the daughter cells. Based on these data, *ergΔ* cells did not exhibit any obvious perturbation of the actin cytoskeleton organization, indicating that the sterol function is likely to be independent of the actin requirement.

*Ste2p Is Neither Hyperphosphorylated nor Ubiquitinated in *ergΔ* Cells*

Ste2p hyperphosphorylation and ubiquitination are prerequisites for pheromone internalization by receptor-mediated endocytosis (Hicke and Riezman, 1996; Hicke *et al.*, 1998). To determine whether *Ste2p* can acquire these modifications in plasma membranes with an aberrant sterol composition, mutant and WT cells were shifted to 37°C, treated with cycloheximide to inhibit receptor synthesis, and α -factor was added. Proteins were extracted from equal amounts of cells before (0 min) and after exposure to α -factor (8 and 16 min) and examined by Western blot analysis with a *Ste2p* antiserum (Figure 3). In agreement with previous reports

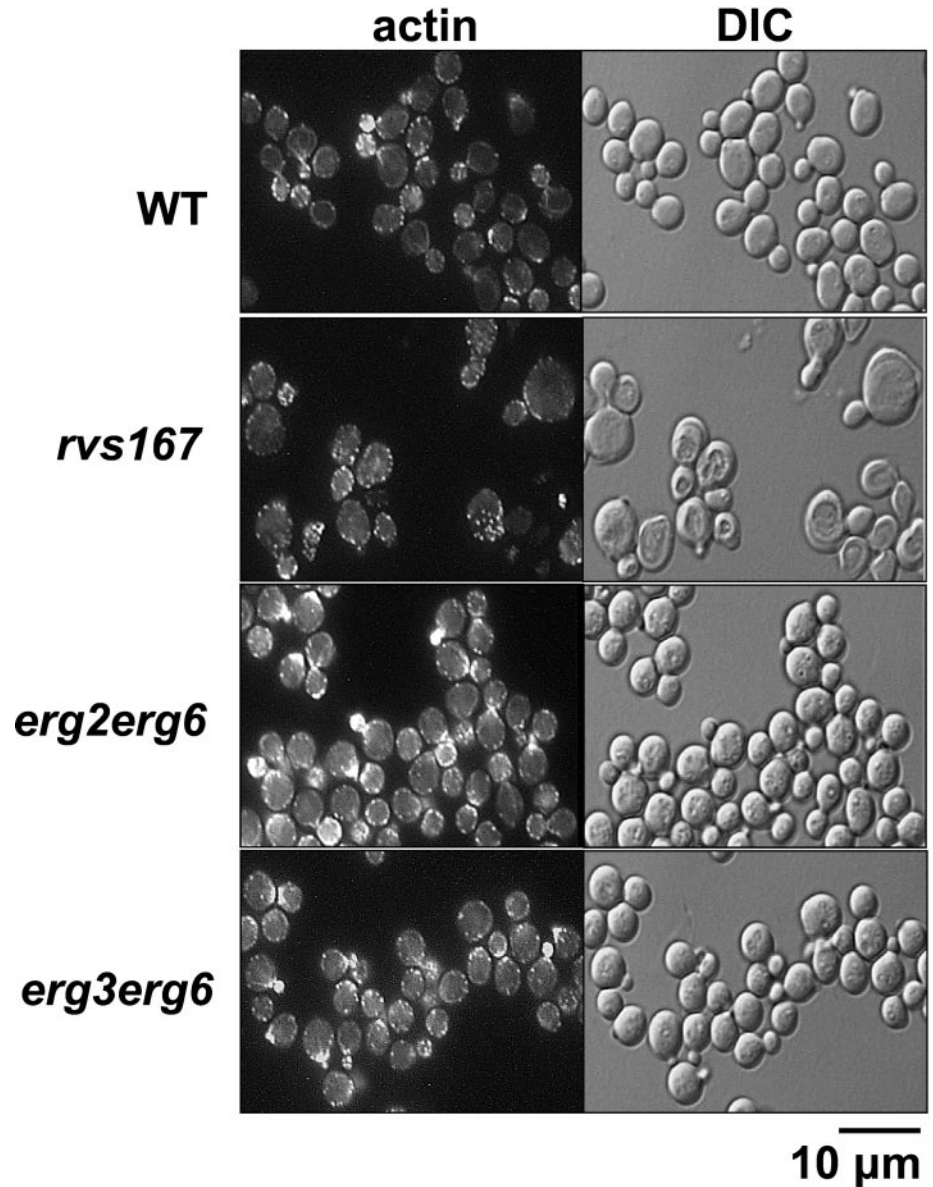


Figure 2. Actin distribution is normal in *ergΔ* cells. Wild-type (WT, RH448), *rvs167Δ* (RH2950), *erg2Δerg6Δ* (RH3616), and *erg3Δerg6Δ* (RH5225) cells were grown at 24°C to early log phase, shifted to 37°C for 2.5–3 h, fixed, stained with rhodamine-phalloidin, and observed by fluorescence (F-actin; left) and Nomarski optics (right).

(Hicke *et al.*, 1998), in the absence of ligand, Ste2p migrated as a doublet in WT cells. On addition of α -factor, these Ste2p species gradually disappeared, and several new ones were detected with a decreased mobility (Figure 3). These Ste2p species correspond to hyperphosphorylated receptor (Hicke *et al.*, 1998). Although it was difficult to visualize the ubiquitinated forms in WT cells (Figure 3) (Hicke and Riezman, 1996), these high molecular mass species could be clearly detected in *rvs167Δ* cells, which accumulate modified Ste2p at the cell surface. A similar phenotype has been previously reported for *end4Δ* cells (Hicke and Riezman, 1996). As a negative control for receptor phosphorylation (Hicke *et al.*, 1998; Feng and Davis, 2000b), α -factor addition did not lead to hyperphosphorylation and ubiquitination of Ste2p in *yck1Δ yck2-2 (yck-ts)* cells lacking functional yeast casein kinase I homologs (Yck1p and Yck2p) at nonpermissive

temperature. These kinases are required for Ste2p phosphorylation and internalization, but not for fluid-phase endocytosis (Hicke *et al.*, 1998; Friant *et al.*, 2000). In additional control experiments, none of the Ste2p species, modified or unmodified, were detected in *ste2Δ* cells.

In agreement with their ability to internalize α -factor (Figure 1), exposure of *erg3Δ* (Figure 3) and *erg4Δerg5Δ* cells (our unpublished observations) to pheromone led to receptor modifications similar to those observed in WT cells. In contrast, in *erg2Δerg6Δ* and *erg3Δerg6Δ* cells (Figure 3), addition of α -factor did not lead to any major change in Ste2p mobility because a doublet with a similar migration was present before and after exposure to α -factor. Longer exposures of the Western blot did not reveal any significant amount of hyperphosphorylated or ubiquitinated Ste2p forms in these mutants. These results show that ligand-

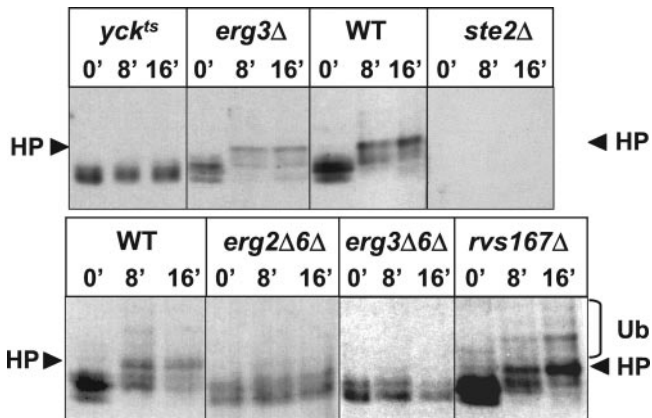


Figure 3. Ste2p is neither hyperphosphorylated nor ubiquitinated in *ergΔ* cells. Wild-type (WT, RH448), *ste2Δ* (RH1298), *yck-ts* (RH3589), *erg3Δ* (RH4213), *rvs167Δ* (RH2950), *erg2Δerg6Δ* (RH3616), and *erg3Δerg6Δ* (RH5225) cells were incubated in the absence (0') or presence of α -factor for 8 or 16 min (8' or 16', respectively) at 37°C. Total proteins were extracted and analyzed for Ste2p by protein blot analysis by using anti-Ste2p antiserum. Ub, ubiquitinated Ste2p indicated by bracket; HP, hyperphosphorylated Ste2p indicated by arrow.

induced receptor modification is defective in the *ergΔ* mutants that exhibit a block in pheromone internalization.

Ste2p Is Present at Plasma Membrane in *ergΔ* Cells

Hyperphosphorylation and ubiquitination of Ste2p are expected to occur at the plasma membrane. Although we demonstrated that the transport of various marker proteins through the secretory pathway is not affected in *ergΔ* cells (Munn *et al.*, 1999) (see below), we wanted to eliminate the possibility that the deficiency in Ste2p modification was merely due to mislocalization of Ste2p. For this purpose, we determined Ste2p localization in *ergΔ* and WT cells before addition of α -factor (Figure 4). After 15-min preshift to 37°C (and thus comparable with the 0-min time point in Figure 3), cells were fixed, and Ste2p was detected by immunofluorescence. As shown previously (Hicke *et al.*, 1997), Ste2p was present at the plasma membrane in WT cells, displaying a ring-like cell-surface labeling. Ste2p was also found in small dot-like structures that have been previously shown to be intracellular and may represent Ste2p that is constitutively internalized or present in the secretory compartment on its way to the cell surface (Hicke *et al.*, 1997). In control experiments, nearly no labeling was observed in *ste2Δ* cells, even when exposed for longer times, confirming the specificity of the antibody. As expected, Ste2p was found at the cell surface in *rvs167Δ* cells. It is noteworthy that despite the strong internalization defect determined by α -factor uptake assays (Munn *et al.*, 1995) in *rvs167Δ* cells, Ste2p was also present in small dot-like structures, suggesting that much of the internal labeling may be receptors on the exocytic pathway under these conditions.

In *erg2Δerg6Δ* and *erg3Δerg6Δ* cells, Ste2p was localized at the plasma membrane because they displayed a similar ring-like surface labeling of Ste2p as observed in WT cells. Mutant *erg2Δerg6Δ* cells also contained small dot-like struc-

tures, which were larger in *erg3Δerg6Δ* cells. This type of labeling is reminiscent of late endosomal staining because the labeled structures reside adjacent to vacuoles (Figure 4) (Hicke *et al.*, 1997). Thus, in addition to an internalization defect, *erg3Δerg6Δ* cells may either exhibit a block at a postinternalization step (see below) or target some portion of the receptor directly to the vacuole without attaining the plasma membrane. In any event, these results demonstrate that in *ergΔ* cells, a considerable amount of Ste2p is localized at the plasma membrane.

α -Factor Binds with Similar Affinity to Ste2p in *ergΔ* Cells and WT Cells

We further investigated whether in *ergΔ* cells, Ste2p modification and subsequent internalization was impaired because of the inability of α -factor to bind to Ste2p. In the α -factor uptake assays (Figure 1) (Dulic *et al.*, 1991), we observed that the ligand was capable of binding to Ste2p in *ergΔ* cells. Furthermore, addition of α -factor induced cell cycle arrest and morphological changes in *ergΔ* cells (our unpublished observations), indicating that the mating response was initiated (Riezman, 1998). To obtain information about the quality of Ste2p-pheromone interaction, WT and *ergΔ* cells were incubated with a fixed amount of radiolabeled α -factor and a varying amount of competitor unlabeled α -factor. Cells were collected and washed, and bound radioactive ligand was determined by scintillation counting. As shown in Figure 5, *erg3Δerg6Δ* cells displayed a similar competition curve as WT cells, providing evidence that α -factor was able to bind to Ste2p with normal affinity in a membrane environment where Ste2p was not hyperphosphorylated, ubiquitinated, or internalized. Similar results were obtained for *erg2Δerg6Δ* and *erg3Δ* cells (unpublished observations). These results suggest that the defect in Ste2p modification and subsequent internalization is not due to the inability of α -factor to bind to Ste2p.

ergΔ Cells Exhibit a Postinternalization Defect in Fluid-Phase Endocytosis

Previously, we observed that in addition to their Ste2p-internalization defects, *erg2Δ* and *erg2Δerg6Δ* cells exhibit a strong defect in fluid-phase endocytosis of the water-soluble dye LY (Munn *et al.*, 1999). To determine whether in *ergΔ* strains, the internalization defect can be correlated with a LY defect, we analyzed the *ergΔ* cells created in the present studies for LY accumulation in their vacuoles (Figure 6). As for receptor-mediated endocytosis (Figure 1), LY accumulation was significantly reduced in *erg2Δerg3Δ* and *erg3Δerg6Δ* cells, with the latter having the most severe defect. Interestingly, *erg3Δ* cells were also unable to accumulate LY in their vacuoles, even although these mutant cells internalized α -factor with WT kinetics (Figure 1). Compared with WT cells, *erg4Δerg5Δ* cells also consistently accumulated less LY in their vacuoles. Lack of LY accumulation was not due to vacuolar fragmentation present in some *ergΔ* cells (see below) because these *ergΔ* strains exhibited reduced LY levels in their unfragmented, larger vacuoles as well (Figure 6) (Munn *et al.*, 1999). It should be noted, however, that LY accumulation allows qualitative rather than quantitative assessment of fluid-phase endocytosis (Dulic *et al.*, 1991). In

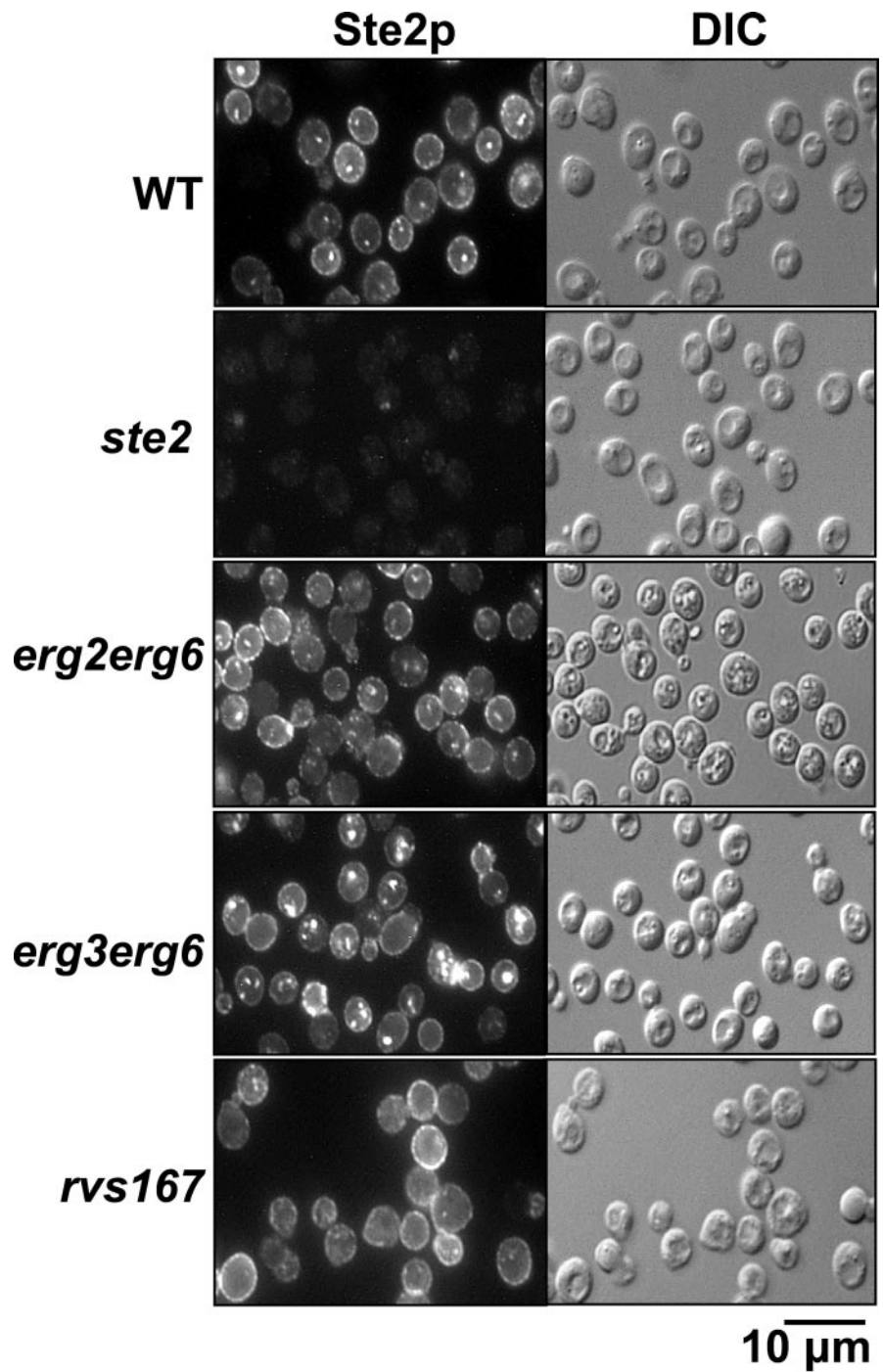


Figure 4. Ste2p is present at the plasma membrane in *ergΔ* cells. The localization of Ste2p was determined in wild-type (WT, RH448), *ste2Δ* (RH1298), *rvs167Δ* (RH2950), *erg2Δerg6Δ* (RH3616), and *erg3Δerg6Δ* (RH5225) cells by immunofluorescence microscopy by using Ste2p antiserum (left) or by Nomarski optics (right).

addition, this assay does not allow differentiation of an internalization vs. a postinternalization defect.

We therefore used the lipophilic styryl dye FM4-64 to investigate the endocytic defect in *ergΔ* cells in more detail. This dye intercalates into membranes, and its fluorescence is greatly enhanced in lipid environments (Betz *et al.*, 1996). In yeast, it is internalized in a time- and energy-dependent manner and labels smaller endocytic compartments and the

vacuole (Vida and Emr, 1995; Wiederkehr *et al.*, 2000). To examine membrane movement from the plasma membrane through the endocytic compartment to the vacuole, we used a pulse-chase labeling experiment in which *ergΔ* and WT cells were incubated with FM4-64 and then washed, and the dye subsequently chased for 15, 30, 45, and 180 min (Figure 7). For a more complete analysis, we included *erg2Δ* and *erg6Δ* cells. In WT cells, small dot-like and perivacuolar

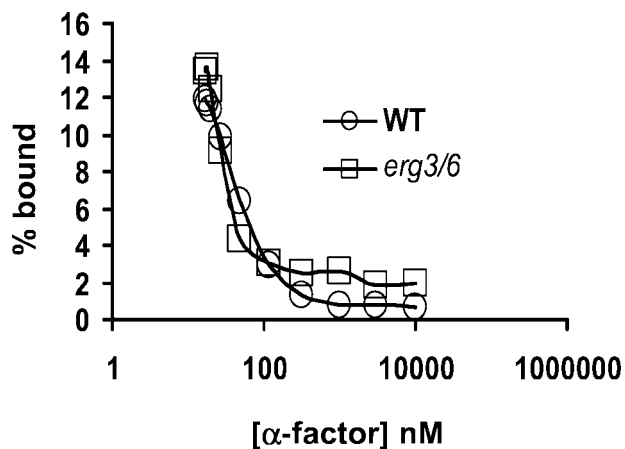


Figure 5. In *erg* Δ cells, α -factor binds to Ste2p with normal affinity. [35 S]- α -factor was bound to wild-type (WT, RH448; circles) or *erg3 Δ erg6 Δ* (*erg3/6*, RH5225; squares) cells in the presence of increasing concentrations of unlabeled α -factor. The percentage of input cpm of [35 S]- α -factor that was bound is plotted vs. the total α -factor concentration.

structures, most likely representing the endosomal and pre-vacuolar compartments, respectively, were visible after 15-min chase. Importantly, *erg* Δ cells showed strong FM4-64 labeling of internal structures after 15-min chase. No uptake could be detected under these conditions in the *end3 Δ* mutant strain, which has an internalization defect (Raths *et al.*, 1993). Therefore, none of the *erg* Δ mutants seems to have a strong internalization defect. After 30 min chase, all strains, with the exception of *end3*, had internal FM4-64 fluorescence. In wild-type cells the vacuole was clearly labeled, but not in *erg* Δ strains. This implies a postinternalization defect in the endocytic pathway in strains with altered sterol composition, consistent with the LY accumulation defect (Figure 6). Surprisingly, in *erg6 Δ* and *erg3 Δ erg6 Δ* cells, at this and later time points, FM4-64 staining was found at the cell periphery. Because there was much less surface FM4-64 staining after 15-min chase, this material may have been recycled from the cell interior. These results suggest an increase in recycling of endocytic content in *erg6 Δ* mutants, but it will be necessary to confirm more carefully whether this dye is really in the plasma membrane.

For all analyzed *erg* Δ strains, FM4-64 labeling of vacuolar membranes was observed after 180-min chase, indicating that FM4-64 transport through the endosomal compartment to the vacuoles was not completely blocked. In agreement with a previous study reporting an ergosterol requirement for homotypic vacuolar fusion (Kato and Wickner, 2001), FM4-64 staining showed that *erg* Δ cells contained fragmented vacuoles with *erg2 Δ* cells having the strongest fragmentation phenotype. One exception was the *erg6 Δ* strain, which in contrast to previous observations (Kato and Wickner, 2001) contained one to three large vacuoles as in WT cells.

In *erg3 Δ* and *erg6 Δ* , FM4-64 transport seemed to be mildly affected because dye movement from the intracellular structures to the vacuole was slightly slower compared with WT cells. Of the single mutant strains, *erg2 Δ* cells exhibited the most obvious defect in FM4-64 movement. Throughout the

time course, but particularly apparent at the 30- and 45-min time points, the dye was present in hazy cellular structures that were never observed in WT cells. These hazy structures could represent small vesicles that are not resolved by light microscopy and are unable to fuse with endocytic compartments. In *erg2 Δ* cells, FM4-64 labeling of the highly fragmented vacuoles was strongly delayed compared with WT cells (compare 180- to 30-min time point, respectively). In all analyzed *erg* Δ double mutant cells, FM4-64-labeled structures, with a similar hazy appearance as those present in *erg2 Δ* cells, were visible during the 15- to 45-min chase. Compared with WT cells, transport of FM4-64 was clearly delayed in *erg2 Δ erg3 Δ* , *erg3 Δ erg6 Δ* , and *erg4 Δ erg5 Δ* cells (compare 30- and 45-min time points). Particularly in *erg4 Δ erg5 Δ* cells, this transport defect seemed to be as pronounced as in *erg2 Δ* cells. Thus, sterols accumulating in *erg2 Δ* , *erg2 Δ erg3 Δ* , *erg3 Δ erg6 Δ* , and *erg4 Δ erg5 Δ* cells were sufficient to support internalization of the membrane-intercalating dye FM4-64, but affected at least one postinternalization step. We did not quantify the amount of internalized FM4-64 that accumulated in the various *erg* Δ strains because the different mutant strains bound quite different amounts of the styryl dye probably due to their altered membrane properties.

erg Δ Mutations Do Not Affect Maturation of Gas1p

Based on analysis of carboxypeptidase Y maturation and secretion of invertase, vesicular trafficking through the secretory pathway is not affected in *erg* Δ mutants whose sterols are unable to support Ste2p internalization (Munn *et al.*, 1999; our unpublished observations). Herein, we examined the endoplasmic reticulum (ER)-to-Golgi transport of Gas1p, a glycosylphosphatidylinositol (GPI) anchored protein located in the plasma membrane, because a recent study has implicated lipid rafts in this transport step (Bagnat *et al.*, 2000). According to the "raft hypothesis," sterols and sphingolipids assemble laterally to form tightly packed lipid rafts that recruit distinct proteins while excluding others and function in membrane trafficking and signaling (Brown and London, 1998; Simons and Ikonen, 2000). Inhibition of sphingoid base and ceramide synthesis blocks transport of GPI-anchored proteins to the Golgi compartment (Horvath *et al.*, 1994; Sutterlin *et al.*, 1997). In addition, at least two types of ER-derived vesicles exist in yeast that carry different cargo from the ER to the Golgi (Muniz *et al.*, 2001). To determine whether a change in sterol composition interfered with Gas1p transport, we monitored the conversion of Gas1p from its core glycosylated ER form (105 kDa) to the mature Golgi form (125 kDa) in *erg* Δ and WT cells. Pulse-chase labeling experiments at 37°C followed by immunoprecipitation of Gas1p showed that Gas1p was matured at similar rates in wild-type and *erg3 Δ erg6 Δ* cells (Figure 8A). Similar data were obtained for *erg2 Δ* and *erg3 Δ* cells (our unpublished observations). These results showed that *erg* Δ cells, which were unable to modify Ste2p and which showed clear defects at a postinternalization step of endocytosis, were fully competent for GPI-anchored protein transport from the ER to the Golgi apparatus.

In the absence of sterols, cold detergent-insoluble proteins (including GPI-anchored proteins) have been reported to become soluble when exposed to nonionic detergent such as Triton X-100 at 4°C (Brown and London, 1998; Bagnat *et al.*,

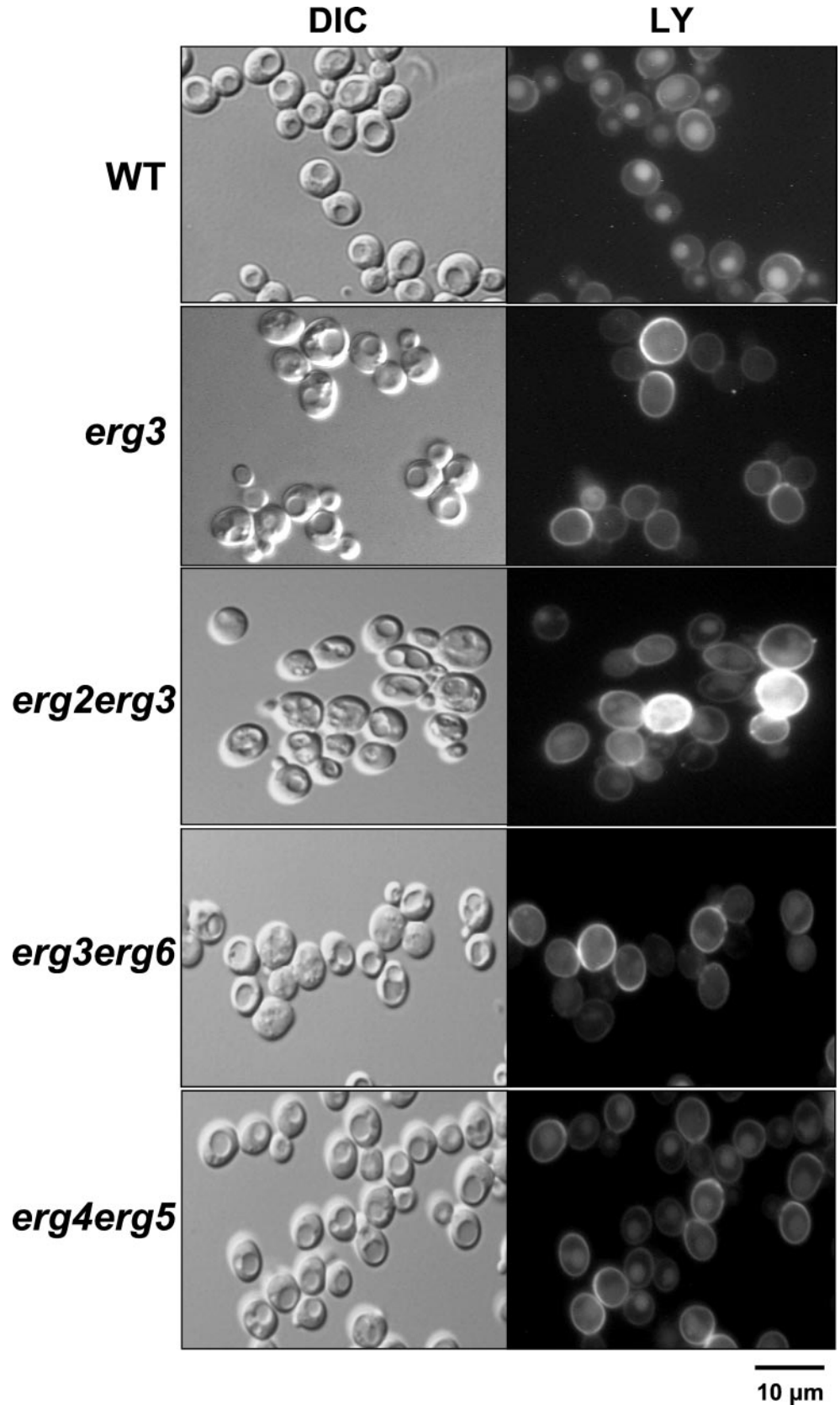


Figure 6. *erg* Δ cells exhibit a defect in LY accumulation. Wild-type (WT, RH448), *erg3* Δ (RH4213), *erg2* $\Delta*erg3* Δ (RH5228), *erg3* $\Delta*erg6* Δ (RH5225), and *erg4* $\Delta*erg5* Δ (RH5233) cells were assayed for fluid-phase endocytosis by visualizing the accumulation of LY in the vacuoles at 24°C. The same field of cells were viewed by fluorescence (right) and by Nomarski optics (left).$$$

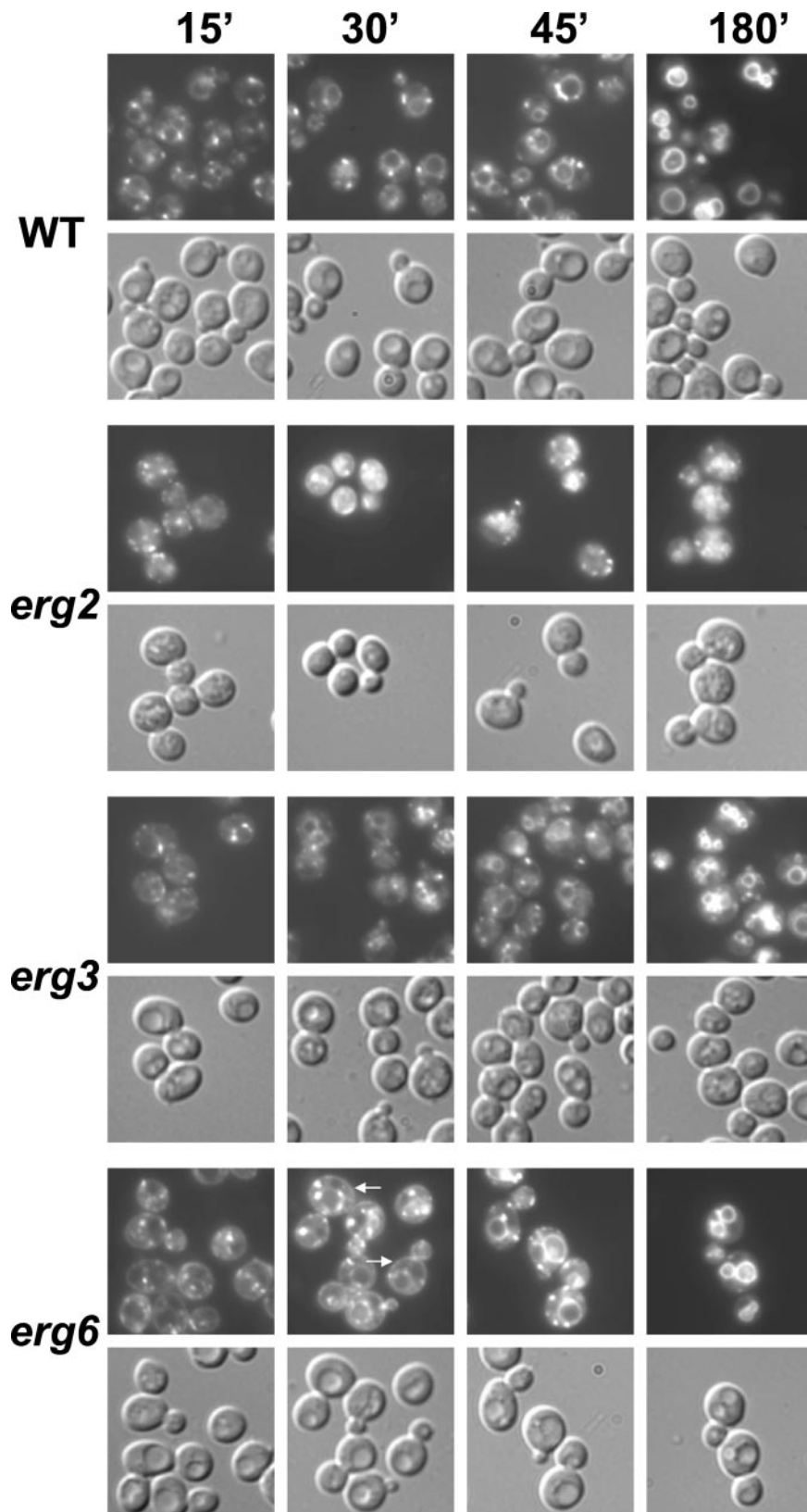


Figure 7. Postinternalization step of endocytosis is affected in *ergΔ* cells. Wild-type (WT, RH448), *erg2Δ* (RH2897), *erg3Δ* (RH4213), *erg6Δ* (RH3622), *erg2Δerg3Δ* (RH5228), *erg3Δerg6Δ* (RH5225), *erg4Δerg5Δ* (RH5233), and *end3Δ* (RH5297) cells were assayed for endocytosis of FM4-64 at 24°C. Internalization and intracellular transport were monitored at 15, 30, 45, and 180 min in a pulse/chase experiment. The same field of cells was viewed by fluorescence (top) and Nomarski optics (bottom).

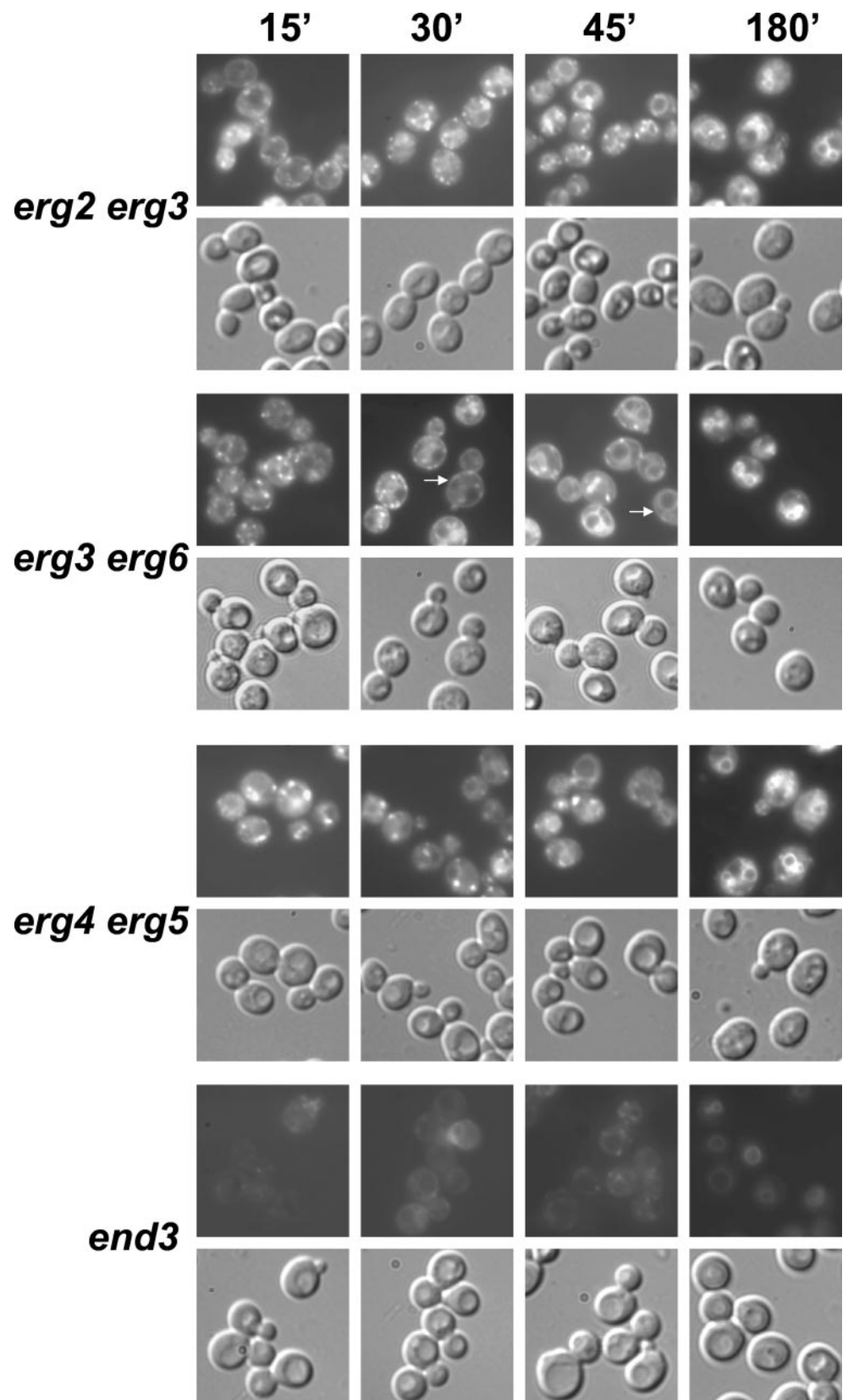


Figure 7 (legend on facing page).

2000). Therefore, we compared the behavior of Gas1p in *ergΔ* mutant and WT cells under steady-state conditions after incubating cell extracts for 1 h on ice in the absence or presence of cold 1% Triton X-100 (Figure 8B). In WT cells, Gas1p was only partially extracted by 1% Triton X-100, but exposure of *erg3Δerg6Δ* cell extract to detergent led to nearly complete solubilization of Gas1p. Interestingly, however, Gas1p was also solubilized to a similar extent in *erg3Δ* as in *erg3Δerg6Δ* cell extracts. Therefore, Gas1p solubility may correlate with the postinternalization defect in endocytosis, but neither with the defect in Ste2p modification nor with GPI-anchored protein transport from the ER to the Golgi apparatus.

DISCUSSION

Using a limited number of *ergΔ* strains, we have previously shown that specific sterol structures are necessary for receptor-mediated and fluid-phase marker endocytosis (Munn *et al.*, 1999). These studies did not tell us, however, whether sterol structures are required at multiple steps and whether the sterol structural requirements are the same for different processes. Therefore, we extended our endocytic analysis by using additional *ergΔ* strains, each accumulating sterols with distinct structural differences to ergosterol and an additional endocytic marker that permits analysis of postinternalization steps. We provide evidence that there are multiple roles for sterols in yeast endocytosis. First, specific sterols are required in receptor-mediated endocytosis at or before receptor hyperphosphorylation arguing for a specific role at an early step in the process. Second, based on experiments analyzing FM4-64 and LY accumulation, sterol structures also have a role at a postinternalization step, which seems to be general. Third, some *ergΔ* mutants show a fragmented vacuole. As discussed below, the sterol structural requirements for these processes are different.

In contrast to most known endocytic factors necessary for ligand-induced Ste2p-internalization, sterol structures are required before or at receptor modification. Based on the ligand competition studies, sterol structures seem to function subsequent to ligand-receptor interaction because changes in the sterol composition did not impair Ste2p function with regard to its ability to bind α -factor. Ste2p was also able to undergo a conformational change because exposure of α -factor induced the mating response (our unpublished observations). We cannot, however, exclude the possibility that aberrant sterols can support conformational changes leading to signaling, but not to receptor hyperphosphorylation.

In *erg2Δerg6Δ* and *erg3Δerg6Δ* cells, whose aberrant sterols did not support α -factor internalization, Ste2p was not significantly hyperphosphorylated in response to binding of the pheromone. Hyperphosphorylation of serine/threonine residues in the cytoplasmic tail of Ste2p is a prerequisite for subsequent ubiquitination, the actual internalization signal (Hicke *et al.*, 1998; Shih *et al.*, 2000). The only kinases known to be involved in receptor phosphorylation are the redundant yeast casein kinase I homologs Yck1p and Yck2p. Similar to sterols, Yck proteins act early in receptor-mediated internalization because in *yck-ts* cells, Ste2p is not internalized due to lack of hyperphosphorylation and ubiquitination after exposure to α -factor (Hicke *et al.*, 1998; Feng and Davis,

2000b). Therefore, the endocytic internalization phenotypes of these *ergΔ* mutants and *yck-ts* cells (Friant *et al.*, 2000) are the same. They are defective in receptor-mediated endocytosis, due to a lack of receptor modification, but competent for the internalization step itself. One possible explanation for the lack of receptor phosphorylation in these *ergΔ* mutants could be the inability to recruit the Yck kinases to their site of action at the plasma membrane. It is not yet known whether these kinases directly phosphorylate Ste2p.

Not all endocytic *ergΔ* phenotypes can be explained by impairment of Yck kinase function because *yck-ts* cells are not defective in fluid-phase endocytosis (Friant *et al.*, 2000). Changes in sterol composition affected both receptor-mediated and fluid-phase endocytosis in *erg2Δ*, *erg2Δerg6Δ*, *erg2Δerg3Δ*, and *erg3Δerg6Δ* cells (this study) (Munn *et al.*, 1999). Importantly, the *erg3Δ* and *erg4Δerg5Δ* cells displayed no defect in receptor-mediated endocytosis enabling us to separate the sterol requirement for receptor modification from a second requirement at a postinternalization step of endocytosis. More specifically, *erg4Δerg5Δ* cells were capable of internalizing FM4-64, but exhibited a delay in postinternalization movement of this membrane marker to vacuoles. It is noteworthy that the sterol structural requirement for fluid-phase endocytosis of a water-soluble dye may be different than that of a membrane-intercalating dye because *erg3Δ* cells exhibited a strong defect in LY accumulation, but transport of FM4-64 was only slightly affected. The opposite results were seen for *erg4Δerg5Δ* cells. In agreement with a postinternalization defect, we observed accumulation of larger dot-like structures in *erg3Δerg6Δ* cells that contained Ste2p and were reminiscent of late endosomes (Figure 4). These structures were not as conspicuous in WT cells. Based on FM4-64 and LY data, the sterol requirement for postinternalization is likely to affect all endocytic traffic.

To determine whether the sterol requirements for the endocytic processes are different, we extended our initial analysis (Munn *et al.*, 1999) in correlating the endocytic defects with the structural changes in the sterol molecule. As shown in Table 2, each *ergΔ* strain accumulated a distinct set of sterols that differed from ergosterol in specific structural features. For clarity, the structures of the most abundant sterols (>10%) of each strain are shown with the observed endocytic phenotypes (Figure 9). The predominant sterol in WT cells was ergosterol (Table 2), a sterol containing two double bonds in the B-ring at C-5,6 and C-7,8, a double bond at C-22,23, and a methyl group (C-28) on C-24 in the side chain (Figure 9). Based on the endocytic phenotypes and sterol analyses of *erg2Δ*, *erg6Δ*, and *erg2Δerg6Δ*, we suggested that the desaturation of the B-ring, but not the side-chain methylation at C-24,28, is critical for internalization of Ste2p (Munn *et al.*, 1999). More specifically, a single double bond at C-8,9 was not sufficient to support receptor internalization, whereas two double bonds, at C-5,6 and C-7,8 or C-8,9, allowed internalization. If the previous suggestions were true then *erg2Δerg3Δ* cells, which accumulated only sterols with a single C-8,9 desaturation, all of which contained a methyl or methenyl group on C-24, would be expected to exhibit a strong block in receptor-mediated internalization as reported for *erg2Δerg6Δ* cells (Munn *et al.*, 1999). However, *erg2Δerg3Δ* cells exhibited only partially reduced α -factor internalization. These results suggest that B-ring desaturation is not the sole structural requirement for

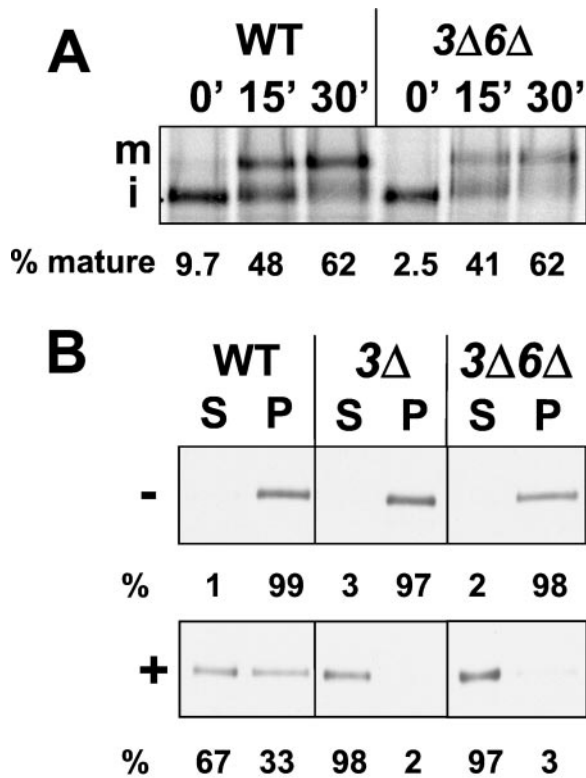


Figure 8. *erg* Δ mutations do not affect maturation of Gas1p, but lead to the solubilization of Gas1p. (A) After a 5-min pulse, Gas1p was immunoprecipitated from wild-type (WT, RH448) and *erg3 Δ erg6 Δ* (3 Δ 6 Δ , RH5225) cells taken at specified time points of chase (minutes). The immunoprecipitates were resolved on 7.5% SDS-PAGE and visualized and quantified on a PhosphorImager. m, mature; i, immature. (B) Wild-type (WT, RH448), *erg3 Δ* (3 Δ , RH4213), and *erg3 Δ erg6 Δ* (3 Δ 6 Δ , RH5225) cell extracts were incubated in the absence (-) or presence (+) of 1% Triton X-100 for 1 h on ice and centrifuged into soluble (S) and insoluble (P) fractions. Proteins were separated by SDS-PAGE and analyzed by Western blot analysis by using Gas1p antiserum followed by densitometry.

its internalization. Mutant *erg3 Δ erg6 Δ* cells, which accumulated a mixture of sterols with a single C-7,8 or C-8,9 desaturation lacking methylation on C-24, showed a severe block in α -factor uptake similar to that of *erg2 Δ erg6 Δ* cells (Munn *et al.*, 1999). Thus, a single desaturation at C-7,8 may not be sufficient to drive receptor-mediated internalization in the absence of methylation on C-24.

Based on the ability to take up α -factor with WT rates in *erg3 Δ* and *erg4 Δ erg5 Δ* cells, changes in the sterol composition did not necessarily lead to a Ste2p-internalization defect. Mutant *erg3 Δ* cells, containing sterols with a single desaturation at C-7,8 with proper side-chain methylation were able to support internalization as well as ergosterol. No desaturation in the side-chain (i.e., lack of C-22,23 desaturation) or a single desaturation at C-24,28 (*erg4 Δ erg5 Δ*) instead of at C-22,23 have no or little effect on internalization (also see *erg2 Δ erg3 Δ* sterols). Although we cannot exclude a role of minor sterols, we conclude that contrary to our previous interpretation (Munn *et al.*, 1999), a combination of both proper B-ring desaturation and side-chain methylation is

most likely required for efficient ligand-induced Ste2p-internalization. Therefore, the overall structure of the ergosterol molecule seems to be important for this endocytic step.

Interestingly, all cells we analyzed with the *erg6 Δ* mutation showed an increase in peripheral staining of FM4-64 after the dye had been internalized. Although the exact nature of this peripheral staining is not known yet, this suggests that the side chain methylation performed by Erg6p may play an important role(s) in the endocytic pathway. If the increased peripheral staining were due to increased recycling, this would be similar to what has been found in mammalian cells. Internalized GPI-anchored proteins are recycled back to the cell surface more rapidly when cells are depleted of cholesterol (Mayor *et al.*, 1998).

In contrast to receptor-mediated internalization, the structural sterol requirements for FM4-64 internalization were more difficult to define because all *erg* Δ strains internalized the dye well. As particularly evident when comparing the endocytic phenotypes for *erg4 Δ erg5 Δ* cells (Figure 9), the structural requirements for internalization and postinternalization steps of fluid-phase endocytosis were different. A change in a single desaturation of the side chain from C-22,23 (present in ergosterol) to C-24,28 (present in ergosta-5,7,24-trienol, the most abundant sterol in *erg4 Δ erg5 Δ* cells), led to a strong delay in postinternalization movement of FM4-64 to vacuoles. In contrast, these structural changes had no effect on Ste2p-internalization. The explanation for the role(s) of sterol in postinternalization will obviously be complex and require further analysis.

We also noticed that *erg* Δ cells frequently had fragmented vacuoles consistent with a role of ergosterol in homotypic vacuole fusion (Kato and Wickner, 2001). The ergosterol requirement for vacuole integrity was distinct from the one for receptor modification because the *erg3 Δ erg6 Δ* mutant showed one of the most severe receptor modification defects, but had normal vacuoles, whereas the *erg3 Δ* mutant showed no receptor modification phenotype, but had strongly fragmented vacuoles (Figures 3 and 7). Vacuolar morphology could also indicate a loss of some vacuolar function, for example vacuole acidification. To obtain a crude measure of vacuole acidification we measured quinacrine accumulation in the vacuoles of the *erg* Δ mutant strains. All of the *erg* Δ mutants were able to accumulate quinacrine in their vacuoles, suggesting that there are no major defects in vacuole acidification due to the *erg* Δ mutations (our unpublished observations).

The ability of *erg* Δ cells, even of those displaying a strong defect in Ste2p internalization, to take up the FM4-64 is in agreement with the fact that their actin cytoskeleton organization was not obviously affected as judged by staining of F-actin. This endocytic behavior differentiates the *erg* Δ strains from other known *end* mutants involved in building or regulating the actin cytoskeleton because these *end* mutants are defective in internalization of FM4-64 (D'Hondt *et al.*, 2000). It is therefore unlikely that in yeast, sterols provide a direct or indirect attachment site for the actin cytoskeleton. Consistent with these results, no significant difference in the extractability of Rvs167p, End3p, and End4p, proteins that interact with the actin cytoskeleton and that are required for Ste2p internalization (Geli and Riezman, 1998; D'Hondt *et al.*, 2000) was observed when comparing *erg* Δ mutant and WT cell extracts (our unpublished observations).

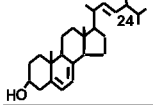
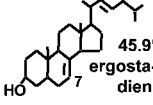
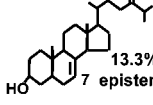
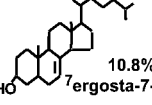
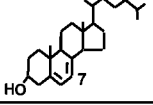
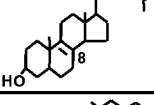
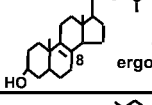
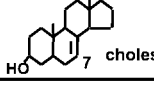
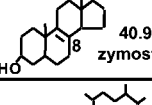
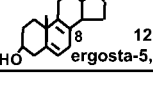
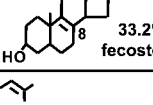
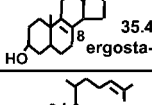
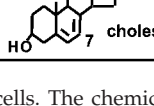
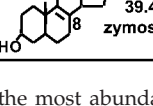
	α -factor internal.	LY uptake	FM4-64 transport	Vacuolar morph.	Sterol Structures
WT	normal	normal	normal	normal	 77% ergosterol
<i>erg3</i> Δ	normal	strongly reduced	slightly delayed	fragmented	 45.9% ergosta-7,22-dienol  13.3% episterol  10.8% ergosta-7-enol
<i>erg4</i> Δ <i>erg5</i> Δ	normal	slightly reduced	delayed	fragmented	 72.2% ergosta-5,7,24-trienol
<i>erg2</i> Δ <i>erg3</i> Δ	reduced	reduced	delayed	strongly fragmented	 39.3% fecosterol  40.4% ergosta-8-enol
<i>erg3</i> Δ <i>erg6</i> Δ	strongly reduced	strongly reduced	delayed	fragmented	 39.5% cholesta-7,24-dienol  40.9% zymosterol
<i>erg2</i> Δ	reduced	strongly reduced	delayed	strongly fragmented	 12.7% ergosta-5,8,22-trienol  33.2% fecosterol  35.4% ergosta-8-enol
<i>erg6</i> Δ	slightly reduced	normal	slightly delayed	normal	 32.3% cholesta-5,7,24-trienol  39.4% zymosterol

Figure 9. Comparison of endocytic phenotypes and sterol structures of *erg* Δ cells. The chemical structures of the most abundant sterols (>10%; as determined in Table 2) were grouped with the different endocytic and vacuolar phenotypes found for wild-type (WT, RH448), *erg2* Δ (RH2897) *erg3* Δ (RH4213), *erg6* Δ (RH3622), *erg2* Δ *erg3* Δ (RH5228), *erg3* Δ *erg6* Δ (RH5225), and *erg4* Δ *erg5* Δ (RH5233) cells. The abundance of each sterol within a strain is given in percentage. internal., internalization.

It is possible that the endocytic defects in *erg* Δ mutant cells may be due to the inability of the aberrant sterols to associate with sphingolipids and thus to organize the lipid environment of the membrane (e.g., “lipid rafts”). We were unable, however, to establish a correlation between detergent solubility of Gas1p, a plasma membrane marker of yeast lipid rafts (Bagnat *et al.*, 2000), and the ability of cells to internalize α -factor. On the other hand, the structural determinants we have identified as important for sterol function in endocytosis are similar to the structural determinants shown to influence sphingolipid/sterol domain formation in model membranes (Xu *et al.*, 2001). These apparently conflicting data could be explained by the association of sterols with different types of lipid rafts or microdomains that coexist in membranes or vary between membranes and exhibit distinct physical properties. If so, it may also provide an explanation for the presence of the different sterol requirements in receptor-mediated and fluid-phase internalization as well as in postinternalization. Alternatively, the *erg* mutations could cause an alteration in the sterol concentration in the plasma membrane, and the different assays, Gas1p solubility and endocytosis, may be affected by different threshold concentrations of sterols. Another possibility is

that the aberrant sterol structures affect the properties of whole bilayers and that the different structural variants of sterols produced in the mutant strains affect the bilayer structures in different ways.

It is also possible that sterols may function in yeast internalization independently of their association with sphingolipids. It should be noted that although suggested (Zanolari *et al.*, 2000), a direct role of sphingolipids in yeast endocytosis has not been demonstrated yet. Clearly, the role of ergosterol differs from that of sphingoid bases, which are sphingolipid precursors recently shown to be required for endocytic internalization (Zanolari *et al.*, 2000). Hyperphosphorylation of Ste2p is not impaired in *lcb1-100* cells defective in sphingoid base synthesis and sphingoid bases are necessary for proper actin cytoskeleton morphology (Zanolari *et al.*, 2000).

Our study provides evidence that ergosterol functions differently in internalization than other previously described components of the yeast endocytic machinery, with the exception of yeast casein kinase I and Akr1p, which is required to recruit casein kinase I to the membrane (Feng and Davis, 2000a). Although many of the other known endocytic factors, including sphingoid bases, act through the actin re-

quirement, ergosterol is important early in Ste2p internalization and sterol function seems to be independent of actin. In addition to receptor hyperphosphorylation, ergosterol is required for postinternalization process(es) in endocytosis, and the availability of a variety of *ergΔ* mutants displaying different endocytic phenotypes will allow us to investigate the roles of sterols in these processes in more detail. It is clear from our data that distinct structural properties of the sterol molecule will be important for its role in the various steps of endocytosis.

ACKNOWLEDGMENTS

We thank the Riezman laboratory for stimulating discussions; A. Alconada for help with making the anti-Ste2p antiserum; J. Holenstein and T. Aust for technical assistance; J. Konopka for a plasmid; and D. Zweyck and E. Leitner for help with the sterol identification and GLC-MS. This work was funded by grants to H.R. from the Swiss National Science Foundation, to A.H.-P. from Human Frontier Science Program and European Molecular Biology Organization, to R.W. from the Uehara Memorial Foundation and Human Frontier Science Program, to H.P. from the Federation of European Biochemistry Societies, and to G.D. from FWF project 14468 and project AUSTROFAN (financially supported by the Austrian Ministry of Education, Science and Culture).

REFERENCES

- Bagnat, M., Keranen, S., Shevchenko, A., and Simons, K. (2000). Lipid rafts function in biosynthetic delivery of proteins to the cell surface in yeast. *Proc. Natl. Acad. Sci. USA* 97, 3254–3259.
- Bard, M., Woods, R.A., Barton, D.H., Corrie, J.E., and Widdowson, D.A. (1977). Sterol mutants of *Saccharomyces cerevisiae*: chromatographic analyses. *Lipids* 12, 645–654.
- Bauer, F., Urdaci, M., Aigle, M., and Crouzet, M. (1993). Alteration of a yeast SH3 protein leads to conditional viability with defects in cytoskeletal and budding patterns. *Mol. Cell. Biol.* 13, 5070–5084.
- Berben, G., Dumont, J., Gilliquet, V., Bolle, P.A., and Hilger, F. (1991). The YDp plasmids: a uniform set of vectors bearing versatile gene disruption cassettes for *Saccharomyces cerevisiae*. *Yeast* 7, 475–477.
- Betz, W.J., Mao, F., and Smith, C.B. (1996). Imaging exocytosis and endocytosis. *Curr. Opin. Neurobiol.* 6, 365–371.
- Brown, D.A., and London, E. (1998). Functions of lipid rafts in biological membranes. *Annu. Rev. Cell Dev. Biol.* 14, 111–136.
- Chang, W.J., Rothberg, K.G., Kamen, B.A., and Anderson, R.G. (1992). Lowering the cholesterol content of MA104 cells inhibits receptor-mediated transport of folate. *J. Cell Biol.* 118, 63–69.
- Corvera, S., D'Arrigo, A., and Stenmark, H. (1999). Phosphoinositides in membrane traffic. *Curr. Opin. Cell Biol.* 11, 460–465.
- Daum, G., Lees, N.D., Bard, M., and Dickson, R. (1998). Biochemistry, cell biology and molecular biology of lipids of *Saccharomyces cerevisiae*. *Yeast* 14, 1471–1510.
- Deckert, M., Tichioni, M., and Bernard, A. (1996). Endocytosis of GPI-anchored proteins in human lymphocytes: role of glycolipid-based domains, actin cytoskeleton, and protein kinases. *J. Cell Biol.* 133, 791–799.
- D'Hondt, K., Heese-Peck, A., and Riezman, H. (2000). Protein and lipid requirements for endocytosis. *Annu. Rev. Genet.* 34, 255–295.
- Dulic, V., Egerton, M., Elguindi, I., Rath, S., Singer, B., and Riezman, H. (1991). Yeast endocytosis assays. *Methods Enzymol.* 194, 697–710.
- Feng, Y., and Davis, N.G. (2000a). Akr1p and the type I casein kinases act prior to the ubiquitination step of yeast endocytosis: Akr1p is required for kinase localization to the plasma membrane. *Mol. Cell. Biol.* 20, 5350–5359.
- Feng, Y., and Davis, N.G. (2000b). Feedback phosphorylation of the yeast α -factor receptor requires activation of the downstream signaling pathway from G protein through mitogen-activated protein kinase. *Mol. Cell. Biol.* 20, 563–574.
- Friant, S., Zanolari, B., and Riezman, H. (2000). Increased protein kinase or decreased PP2A activity bypasses sphingoid base requirement in endocytosis. *EMBO J.* 19, 2834–2844.
- Geli, M.I., and Riezman, H. (1998). Endocytic internalization in yeast and animal cells: similar and different. *J. Cell Sci.* 111, 1031–1037.
- Geli, M.I., Wesp, A., and Riezman, H. (1998). Distinct functions of calmodulin are required for the uptake step of receptor-mediated endocytosis in yeast: the type I myosin Myo5p is one of the calmodulin targets. *EMBO J.* 17, 635–647.
- Grimmer, S., Iversen, T.G., van Deurs, B., and Sandvig, K. (2000). Endosome to Golgi transport of ricin is regulated by cholesterol. *Mol. Biol. Cell* 11, 4205–4216.
- Heiniger, H.J., Kandutsch, A.A., and Chen, H.W. (1976). Depletion of L-cell sterol depresses endocytosis. *Nature* 263, 515–517.
- Hicke, L., and Riezman, H. (1996). Ubiquitination of a yeast plasma membrane receptor signals its ligand-stimulated endocytosis. *Cell* 84, 277–287.
- Hicke, L., Zanolari, B., Pypaert, M., Rohrer, J., and Riezman, H. (1997). Transport through the yeast endocytic pathway occurs through morphologically distinct compartments and requires an active secretory pathway and Sec18p/N-ethylmaleimide-sensitive fusion protein. *Mol. Biol. Cell* 8, 13–31.
- Hicke, L., Zanolari, B., and Riezman, H. (1998). Cytoplasmic tail phosphorylation of the α -factor receptor is required for its ubiquitination and internalization. *J. Cell Biol.* 141, 349–358.
- Horvath, A., Sutterlin, C., Manning-Krieg, U., Movva, N.R., and Riezman, H. (1994). Ceramide synthesis enhances transport of GPI-anchored proteins to the Golgi apparatus in yeast. *EMBO J* 13, 3687–3695.
- Jenness, D.D., Burkholder, A.C., and Hartwell, L.H. (1983). Binding of α -factor pheromone to yeast cells: chemical and genetic evidence for an α -factor receptor. *Cell* 35, 521–529.
- Kato, M., and Wickner, W. (2001). Ergosterol is required for the Sec18/ATP-dependent priming step of homotypic vacuole fusion. *EMBO J.* 20, 4035–4040.
- Keesler, G.A., Casey, W.M., and Parks, L.W. (1992). Stimulation by heme of steryl ester synthase and aerobic sterol exclusion in the yeast *Saccharomyces cerevisiae*. *Arch. Biochem. Biophys.* 296, 474–481.
- Kilmartin, J.V., and Adams, A.E. (1984). Structural rearrangements of tubulin and actin during the cell cycle of the yeast *Saccharomyces*. *J. Cell Biol.* 98, 922–933.
- Konopka, J.B., Jenness, D.D., and Hartwell, L.H. (1988). The C-terminus of the *S. cerevisiae* α -pheromone receptor mediates an adaptive response to pheromone. *Cell* 54, 609–620.
- Kubler, E., and Riezman, H. (1993). Actin and fimbrin are required for the internalization step of endocytosis in yeast. *EMBO J.* 12, 2855–2862.
- Lombardi, R., and Riezman, H. (2001). Rvs161p and Rvs167p, the two yeast amphiphysin homologs, function together in vivo. *J. Biol. Chem.* 276, 6016–6022.

- Mayor, S., Sabharanjak, S., and Maxfield, F.R. (1998). Cholesterol-dependent retention of GPI-anchored proteins in endosomes. *EMBO J.* *17*, 4626–4638.
- Muniz, M., Morsomme, P., and Riezman, H. (2001). Protein sorting upon exit from the endoplasmic reticulum. *Cell* *104*, 313–320.
- Munn, A.L., Heese-Peck, A., Stevenson, B.J., Pichler, H., and Riezman, H. (1999). Specific sterols required for the internalization step of endocytosis in yeast. *Mol. Biol. Cell* *10*, 3943–3957.
- Munn, A.L., and Riezman, H. (1994). Endocytosis is required for the growth of vacuolar H(+)-ATPase-defective yeast: identification of six new END genes. *J. Cell Biol.* *127*, 373–386.
- Munn, A.L., Stevenson, B.J., Geli, M.I., and Riezman, H. (1995). end5, end6, and end7: mutations that cause actin delocalization and block the internalization step of endocytosis in *Saccharomyces cerevisiae*. *Mol. Biol. Cell* *6*, 1721–1742.
- Orlandi, P.A., and Fishman, P.H. (1998). Filipin-dependent inhibition of cholera toxin: evidence for toxin internalization and activation through caveolae-like domains. *J. Cell Biol.* *141*, 905–915.
- Parton, R.G., Joggerst, B., and Simons, K. (1994). Regulated internalization of caveolae. *J. Cell Biol.* *127*, 1199–1215.
- Raths, S., Rohrer, J., Crausaz, F., and Riezman, H. (1993). end3 and end4: two mutants defective in receptor-mediated and fluid-phase endocytosis in *Saccharomyces cerevisiae*. *J. Cell Biol.* *120*, 55–65.
- Reneke, J.E., Blumer, K.J., Courchesne, W.E., and Thorner, J. (1988). The carboxy-terminal segment of the yeast α -factor receptor is a regulatory domain. *Cell* *55*, 221–234.
- Riezman, H. (1998). Down regulation of yeast G protein-coupled receptors. *Semin Cell Dev Biol* *9*, 129–134.
- Rodal, S.K., Skretting, G., Garred, O., Vilhardt, F., van Deurs, B., and Sandvig, K. (1999). Extraction of cholesterol with methyl- β -cyclodextrin perturbs formation of clathrin-coated endocytic vesicles. *Mol. Biol. Cell* *10*, 961–974.
- Rothman, J.H., Yamashiro, C.T., Raymond, C.K., Kane, P.M., and Stevens, T.H. (1989). Acidification of the lysosome-like vacuole and the vacuolar H⁺-ATPase are deficient in two yeast mutants that fail to sort vacuolar proteins. *J. Cell Biol.* *109*, 93–100.
- Schaerer-Brodbeck, C., and Riezman, H. (2000). Functional interactions between the p35 subunit of the Arp2/3 complex and calmodulin in yeast. *Mol. Biol. Cell* *11*, 1113–1127.
- Schmidt, A., Wolde, M., Thiele, C., Fest, W., Kratzin, H., Podtelejnikov, A.V., Witke, W., Huttner, W.B., and Soling, H.D. (1999). Endophilin I mediates synaptic vesicle formation by transfer of arachidonate to lysophosphatidic acid. *Nature* *401*, 133–141.
- Shih, S.C., Sloper-Mold, K.E., and Hicke, L. (2000). Monoubiquitin carries a novel internalization signal that is appended to activated receptors. *EMBO J.* *19*, 187–198.
- Simons, K., and Ikonen, E. (2000). How cells handle cholesterol. *Science* *290*, 1721–1726.
- Smith, S.J., and Parks, L.W. (1993). The ERG3 gene in *Saccharomyces cerevisiae* is required for the utilization of respiratory substrates and in heme-deficient cells. *Yeast* *9*, 1177–1187.
- Subtil, A., Gaidarov, I., Kobylarz, K., Lampson, M.A., Keen, J.H., and McGraw, T.E. (1999). Acute cholesterol depletion inhibits clathrin-coated pit budding. *Proc. Natl. Acad. Sci. USA* *96*, 6775–6780.
- Sutterlin, C., Doering, T.L., Schimmoller, F., Schroder, S., and Riezman, H. (1997). Specific requirements for the ER to Golgi transport of GPI-anchored proteins in yeast. *J. Cell Sci.* *110*, 2703–2714.
- Terrell, J., Shih, S., Dunn, R., and Hicke, L. (1998). A function for monoubiquitination in the internalization of a G protein-coupled receptor. *Mol. Cell* *1*, 193–202.
- Trocha, P.J., and Sprinson, D.B. (1976). Location and regulation of early enzymes of sterol biosynthesis in yeast. *Arch. Biochem. Biophys.* *174*, 45–51.
- Vida, T.A., and Emr, S.D. (1995). A new vital stain for visualizing vacuolar membrane dynamics and endocytosis in yeast. *J. Cell Biol.* *128*, 779–792.
- Wach, A. (1996). PCR-synthesis of marker cassettes with long flanking homology regions for gene disruptions in *S. cerevisiae*. *Yeast* *12*, 259–265.
- Weisman, L.S., Bacallao, R., and Wickner, W. (1987). Multiple methods of visualizing the yeast vacuole permit evaluation of its morphology and inheritance during the cell cycle. *J. Cell Biol.* *105*, 1539–1547.
- Wiederkehr, A., Avaro, S., Prescianotto-Baschong, C., Haguenaer-Tsapis, R., and Riezman, H. (2000). The F-box protein Rcy1p is involved in endocytic membrane traffic and recycling out of an early endosome in *Saccharomyces cerevisiae*. *J. Cell Biol.* *149*, 397–410.
- Xu, X., Bittman, R., Duportail, G., Heissler, D., Vilcheze, C., and London, E. (2001). Effect of the structure of natural sterols and sphingolipids on the formation of ordered sphingolipid/sterol domains (rafts). Comparison of cholesterol to plant, fungal, and disease-associated sterols and comparison of sphingomyelin, cerebroside, and ceramide. *J. Biol. Chem.* *276*, 33540–33546.
- Zanolari, B., Friant, S., Funato, K., Sutterlin, C., Stevenson, B.J., and Riezman, H. (2000). Sphingoid base synthesis requirement for endocytosis in *Saccharomyces cerevisiae*. *EMBO J.* *19*, 2824–2833.